Transverse Traveling Wave Plasma Engine

LEE HEFLINGER,* STUART RIDGWAY,† AND ALLAN SCHAFFER‡
General Technology Corporation, Torrance, Calif.

Experimental performance of a plasma engine shows a strong accelerative coupling between the moving transverse magnetic field and the plasma propellant. There were 160 kw of power transferred to a helium plasma with 50% of this initially appearing as axially directed kinetic energy. However, at present, half of the energy given to the plasma is ultimately lost to the propulsion tube walls causing a serious degrading of the useful efficiency.

Introduction

ELECTRICAL propulsion devices, such as plasma engines and ion engines, are low-thrust rockets, the principal application of which is long duration interplanetary flights. A primary reason for the interest in an induction type plasma engine is the potential advantage in long-term reliability resulting from the complete absence of electrodes in contact with plasma. Another reason is the high propulsive power density available.

The induction plasma engine is in many respects similar to the common induction motor. Both employ traveling magnetic fields without brushes (electrodes), and both derive the coupling force from interactions between the traveling field and currents induced in the armature (plasma). However, the plasma engine is concerned only with the start-up process, i.e., with bringing the plasma armature up to speed. After attaining the desired speed the plasma must be discharged as rapidly as possible in order to minimize losses. The induction engine is thus required to accelerate a continuously fed gaseous armature from essentially rest to, say, 5×10^4 m/sec with good efficiency.

Compared to most other plasma induction engines,[1–4] the present device tends to operate at relatively high gas densities (greater than 10^{20} particles/m^3) and larger effective magnetic field strengths (about 500 gauss). The plasma is a continuum in the sense that the mean free path is small compared to physical dimensions and that $\omega\tau$ of the electrons is small compared to unity so that Hall effects are negligible.

The most distinguishing feature of the present engine, however, is the transverse geometry of the magnetic field; i.e., the direction of the magnetic field is essentially perpendicular to its direction of travel (see Fig. 1). This geometry provides very strong accelerative coupling between the traveling magnetic field and the plasma. Its disadvantage is the difficulty in keeping the plasma from intercepting the tube walls.

In analogy to the ring currents induced in a conducting slab by a time-varying normal magnetic field, the induced current paths in the plasma can be viewed as closed curves lying in the plane perpendicular to the magnetic field vector. The induced current filament is subjected to a net accelerative force when its phase angle relative to that of the driving magnetic field differs from $n\pi/2$.

Engine Description

One version of the engine is shown schematically in Fig. 1. Cold propellant enters at the top, is ionized automatically by the electric field associated with the time-varying magnetic field, and is accelerated downward. This is also the direction of travel of the magnetic field. The magnetic field vector is indicated as perpendicular to this direction.

This traveling transverse field is produced by four pairs of coils having sinusoidal currents with relative phasings of 0°, 90°, 180°, and 270°, respectively. With proper spacing between coil pairs, this arrangement produces a smooth translating transverse field on the centerline of the tube. Standing wave components of the field do exist at the tube walls near the poles. However, in other variations of coil windings which have been tested, virtually all standing wave components have been eliminated by smearing out the coils in space and allowing adjacent coils to overlap.

The electrical power for the drive coils is supplied by a megawatt-level two-phase oscillator operating at 480 kc/sec. One phase supplies the 0° and 180° coils, whereas the other phase supplies the 90° and 270° coils. The two phases are locked at 90° relative phasing by appropriate feedback and phase shift networks (see Fig. 2). Two ITT-type D-1037 vacuum triodes are employed as class C oscillators to feed the tank circuits comprised of the drive coils and resonating capacitors.

Because megawatt power is not available in our laboratory on a steady-state basis, the plate voltage to the oscillator is supplied from a pulse-forming network for a period of 1.25 msec. Steady-state conditions exist during this period, which covers 600 cycles of operation at the frequency 480 kc/sec.

Since the power is supplied as an on-off square wave, the propellant must be supplied in the same manner in order to facilitate performance measurements. The desired wave

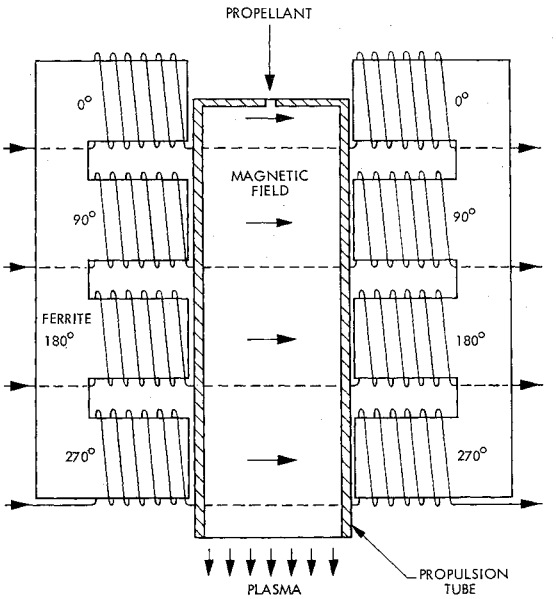

Fig. 1 Schematic of accelerator.

* Senior Scientist; now, Member of the Technical Staff, TRW Space Technology Laboratories, Redondo Beach, Calif.

† Vice President and Technical Director.

‡ Senior Scientist; now Head, Gas Dynamics Section, Aerospace Corp., San Bernardino, Calif. Member AIAA.

form is furnished by the pulsed gas valve shown in Fig. 3. A capacitor discharge is used to dump 400 joules through the pancake coil. Mirror currents induced in the aluminum valve disk produce an impulse, which causes the disk to open. It is closed by the spring. The displacement is thus half of a sine wave. The gas pulse would also be of this form were not the nozzle the prime restriction. The action of the nozzle is to clip the half sine wave so that an approximate square wave is produced. The form of the wave has been checked with a fast ionization gage.[5]

The engine exhausts into a conventional vacuum tank, which simulates outer space. A background pressure of about 10^{-5} torr is maintained, and this typically rises less than an order of magnitude during the 1.25 msec run. The vacuum tank pressure is many orders of magnitude less than the stagnation pressure of the exhaust.

Instrumentation

All performance measurements are made on a time-integrated basis for the entire 1.25 msec run; i.e., measurements are made of the total impulse, the total mass used, and the total energy supplied during the run. The engine is thus penalized for any losses associated with start-up and shutdown of the run.

The electrodeless induction engine affords a unique opportunity to measure directly the net acceleration effect resulting from the Lorentz forces on the plasma. The drive coils are suspended as a pendulum *free* of contact with the propulsion tube, which is itself rigidly attached to the vacuum tank. The drive-coil pendulum (see Fig. 4) can respond only to the back reaction from the net component of the Lorentz forces parallel to the centerline of the propulsion tube. The throw of the pendulum is proportional to the total impulse delivered during the run. A Schaevitz differential transformer is used to measure the throw. Calibration is accomplished by the application of a known impulse, which is delivered by an auxiliary pendulum consisting of a small bob of known mass and visually measurable displacement. Sticky tape is used to insure that the bob sticks to the drive-coil pendulum upon impact, thus insuring that the entire momentum of the bob is precisely transferred to the pendulum.

The total back reaction on the engine consists of the Lorentz force plus forces arising from interactions between the plasma and the tube walls. The drive coil pendulum responds only to the first of these. Therefore, an additional

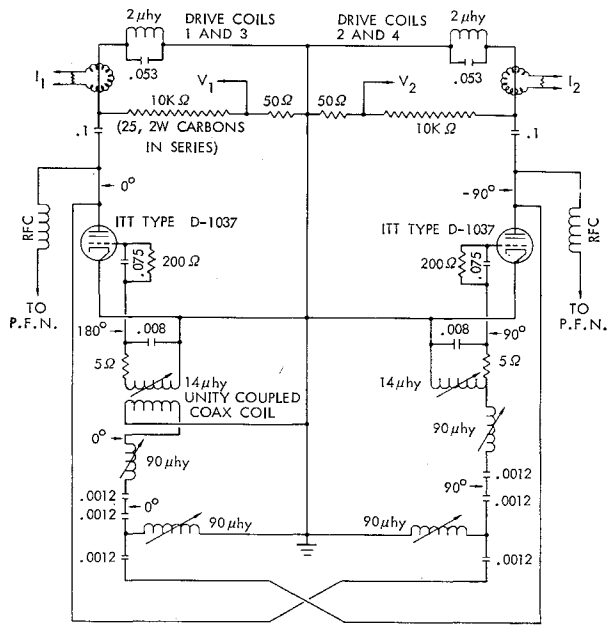

Fig. 2 Two-phase oscillator (all capacitance in microfarads).

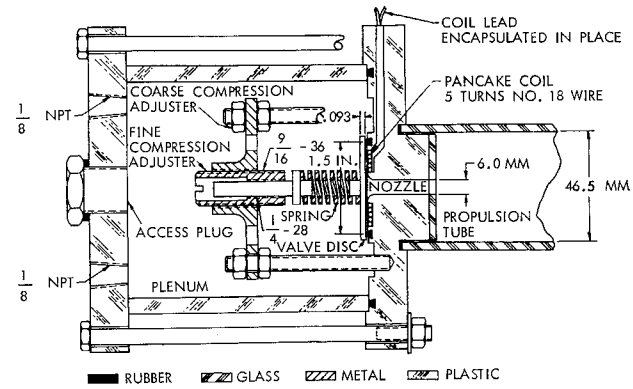

Fig. 3 Pulsed gas valve.

measurement is required to determine the net thrust, and this has been made both by inserting a thrust target into the engine exhaust and by suspending a false tube wall as a pendulum. The false wall is a thin cylindrical liner, which has a diameter slightly less than the tube inside diameter and which is free to move as a pendulum and thus is directly responsive to the wall drag.

The mass utilized by the engine is determined by observing the increase in the ionization gage reading for the vacuum tank during the run. Calibration is accomplished by injecting a precisely known mass of gas from a small auxiliary chamber. Generally, the ionization gage shows about the same reading when the oscillator is fired together with the valve as it does when the valve is fired alone. This observation gives confidence that there are no extraneous mass flows, such as erosion, which are sufficiently serious to affect the performance in short-term tests.

The energy delivered to the plasma is determined by measuring the total energy supplied to the drive coils plus plasma and substracting from this number the coil dissipation at the measured operating voltage. The engine is thus not penalized for the coil losses, since little effort has as yet been made to minimize these. As shown in Fig. 5, the energy measurement is accomplished by means of a Beckman Model 353 thin film Hall multiplier, which is used to multiply the instantaneous current and voltage from the class C oscillator. The output from the Hall device is fed to a ballistic galvanometer, which integrates the instantaneous power to yield the total energy supplied during the 1.25 msec run. Calibration is accomplished by replacing the plasma with a graphite armature and measuring the temperature rise in the graphite directly with thermocouples.

Time-resolved instrumentation is also employed. The relative phasing between the two oscillators is monitored by placing the voltage from one oscillator onto the horizontal plates of an oscilloscope and the voltage from the other onto the vertical plates. The resulting ellipse gives both phase

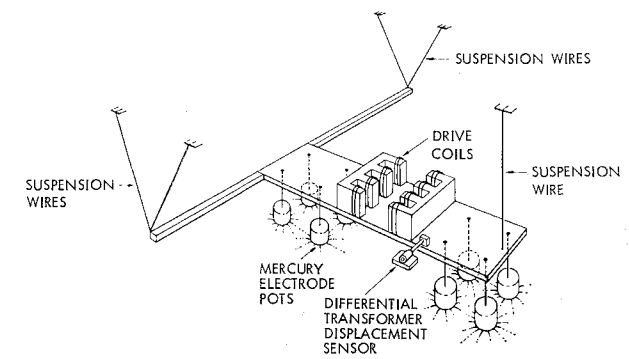

Fig. 4 Drive-coil pendulum.

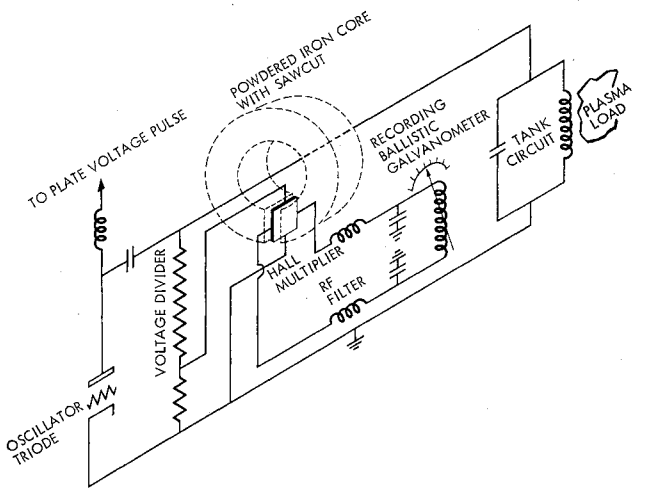

Fig. 5 Circuit for Hall-effect energy meter.

and amplitude information. Light output and tank circuit voltages are also monitored to be certain that a steady state exists during the run.

Elementary Theory

A complete theoretical analysis of the operation of this engine is not feasible because of the combined complexities of the three-dimensional geometry, compressibility effects, high variable conductivity, and intermediate magnetic Reynolds number. Nevertheless, certain significant features can be demonstrated by a very simple analysis.

Assume a two-dimensional magnetic field and armature with the magnetic field vector pointing in the y direction and the field traveling in the z direction at constant-phase velocity. In the orthogonal x direction properties are invariant. Furthermore, let the armature be rigid with uniform conductivity, and let v be the relative velocity between the armature and the traveling field. The coordinate system will be fixed to the armature. Finally, assume the magnetic Reynolds number to be negligibly small; i.e., assume that the induced magnetic field is negligible compared to the applied magnetic field. The magnetic field $\mathbf{B}(y, z)$ will then satisfy $\nabla \times \mathbf{B} = 0, \nabla \cdot \mathbf{B} = 0$.

The desired boundary conditions for the traveling sinusoidal wave are

$$B_z(0,z) = 0 \qquad B_y(0, z) = B_0 \cos[(2\pi/\lambda)(z - vt)]$$

The solution is

$$B_z = -B_0 \sinh[2\pi y/\lambda] \sin[(2\pi/\lambda)(z - vt)]$$
$$B_y = B_0 \cosh[2\pi y/\lambda] \cos[(2\pi/\lambda)(z - vt)]$$

The equation $\nabla \times \mathbf{E} = -(\partial \mathbf{B}/\partial t)$ yields

$$E_z = E_y = 0 \qquad E_x = B_0 v \cosh[2\pi y/\lambda] \cos[(2\pi/\lambda)(z - vt)]$$

In the chosen coordinate system, $\mathbf{j} = \sigma \mathbf{E}$. Finally, for the force per unit volume $\mathbf{f} = \mathbf{j} \times \mathbf{B}$, there results

$$f_z = \sigma B_0^2 v \cosh^2[2\pi y/\lambda] \cos^2[(2\pi/\lambda)(z - vt)]$$
$$f_y = (\sigma B_0^2 v/4) \sinh[4\pi y/\lambda] \sin[(4\pi/\lambda)(z - vt)]$$

The accelerating force f_z is always in the direction of the relative velocity at twice the apparent frequency. The transverse force f_y is considerably weaker than the accelerating force. Moreover, the transverse force alternates its direction inward and outward at twice the apparent frequency. It is not evident whether, in practice, the transverse force will have a net focusing or defocusing effect. It is, of course, desirable that the plasma be focused toward the tube centerline in order to minimize wall interactions. By a qualitative extension of the analysis for a full three-dimensional case, it can also be shown that, in the x direction, the armature is likewise subjected to an alternating force toward and away from the centerline.

The simplified theoretical analysis confirms the expectation of strong coupling in the z direction, but indicates the possible existence of forces tending to drive the plasma toward the walls.

Experimental Results

Data to be presented apply to an engine one wavelength long having four pairs of drive coils each 90° out of phase with its neighbors. The frequency is 480 kc/sec, and the phase velocity is constant at 5.4×10^4 m/sec. The oscillator runs for 1.25 msec, or 600 cycles. The gas valve has an effective pulse length of about 1.45 msec and is actuated 0.2 msec before the oscillator. The propulsion tube is 4.6 cm i.d. The accelerator length from the start of the first drive coil to the end of the last coil is 9.5 cm.

One of the earliest results obtained was that the engine operates in a steady-state manner during the run. Time-resolved diagnostics, such as light output from the plasma and tank circuit voltage, show that the steady state is achieved in about 0.1 msec after oscillator actuation and continues until the 1.25 msec run is terminated. During this time, the gas is continuously admitted to the engine, is ionized spontaneously, is accelerated, and is discharged from the tube exit steadily.

A number of parametric studies have been performed in an attempt to determine the optimum operating conditions. Propellant mass flowrate, type of propellant, magnetic field strength, relative phasing, valve-oscillator relative timing, and coil geometry have been varied.

The propellants tested include helium, neon, argon, hydrogen, nitrogen, and air. Typical performance curves for the various propellants are shown in Fig. 6. The ordinate is the electromagnetic specific impulse defined as the back impulse on the coils divided by g times the mass utilized.§ Substantially the same relative performance results if efficiency is plotted rather than specific impulse. The best perform-

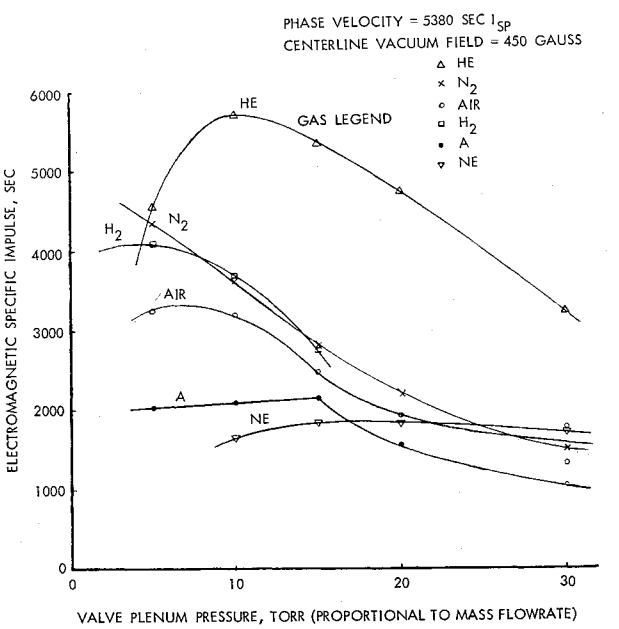

Fig. 6 Performance with various propellants.

§ The electromagnetic specific impulse does not equal the useful specific impulse, since the back impulse on the drive coils is the sum of useful impulse and the wall drag.

ance is obtained using helium, whereas nitrogen is second best. Hydrogen performance is limited by ionization difficulties. Argon suffers from poor mass utilization because of filling and emptying losses associated with the short time duration of the run. Neon exhibits anamolously poor performance. All propellants have an optimum mass flowrate with the optimum number density being in the range 10^{20} to 10^{21} particles/m^3. For helium propellant, the optimum mass flowrate is approximately 5×10^{-5} kg/sec.

Performance increases with increasing magnetic field strength up to fields of about 500 gauss as shown in Fig. 7. Further increases to 700 gauss yielded no increase in performance. Most data were taken at 450 gauss which corresponds to a charging voltage of 25 kv for the pulse-forming network. Performance is an optimum when the relative phasing between the two oscillators is 90°, but variations of 10° or so have little effect. If the phase is adjusted with no plasma present, the perturbation in phasing occasioned by the presence of the plasma is sufficiently small that it causes no difficulty. Performance is generally highest when the gas valve is actuated 0.2 msec before the oscillator, although the timing is not critical.

Performance variations associated with a change from a lumped pole geometry (see Fig. 1) to a distributed pole geometry (with no standing wave components) have been investigated. The optimum performance for the distributed coils occurs at higher power levels and greater thrusts, but the efficiency and relative importance of wall losses is not greatly changed. Performance data to be given are taken from operation with the lumped coil configuration. The distributed coils give approximately 40% higher thrust and power.

The performance of the engine is best displayed by means of an energy balance (see Fig. 8). The data, which have been rounded somewhat, are for a typical run using helium at the optimum operating conditions. The input energy, 200 joules (corresponding to 160 kw), is measured directly, as previously described. The axial kinetic energy KE of 100 joules (corresponding to 80 kw) is computed from the measured drive coil back impulse I and the measured mass utilized M, by the usual performance definition KE = $I^2/(2M)$.¶ The sum of the nonaxial kinetic energy and other losses is obtained by differencing the axial kinetic energy from the input energy. The portion of the axial kinetic energy appearing in the exhaust is determined by a thrust target, whereas the portion going to the walls has been measured

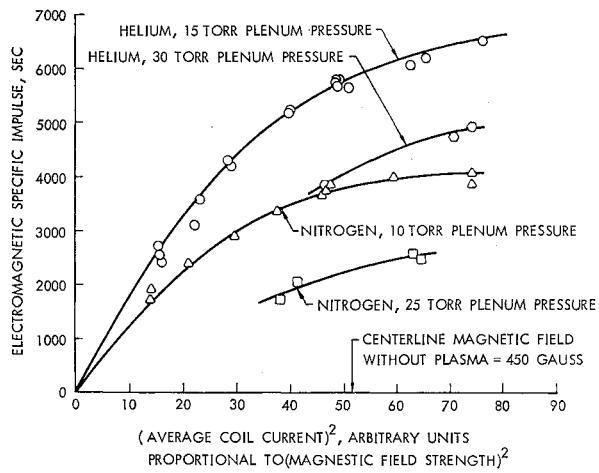

Fig. 7 Effect of varying magnetic field strength.

¶ This formula actually assumes a model described in the next footnote and gives the minimum kinetic energy of mass M which would produce the impulse I. The actual kinetic energy may be higher, depending upon the velocity uniformity.

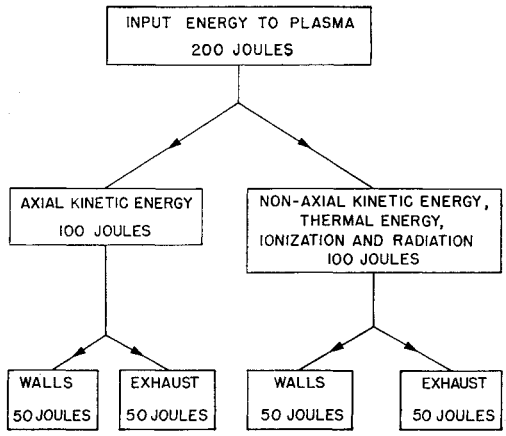

Fig. 8 Energy flow diagram.

with a false wall pendulum.** Calorimetric measurements of the total energy given to the tube walls and the total energy in the exhaust enable the energy balance to be completed.

The calorimetric measurement of the energy lost to the tube walls is accomplished by attaching thermocouples to the outside of the pyrex propulsion tube and noting the temperature rises at various stations after the 1.25 msec run. A typical result is shown in Fig. 9. This curve is, subsequently, spatially integrated to obtain the total heat lost to the walls. The energy in the exhaust is taken to be that which is caught in a bag-type copper calorimeter plus that transferred to the tube walls in the region downstream of the accelerating coils, since in an actual engine this extra tubing (used for connecting to the vacuum tank) would be removed.

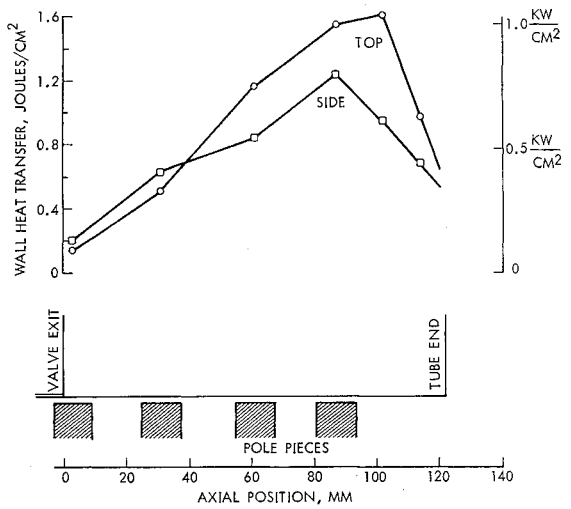

Fig. 9 Heat input to propulsion tube wall.

** The actual measurements showed that the impulse in the exhaust approximately equaled the impulse lost to the tube walls and that the sum of these two approximately equaled the back reaction on the drive coils. For the purposes of the energy balance, it was inferred from these results that half of the input axial kinetic energy is lost to the tube walls and half appears in the exhaust. This interpretation is based on a model in which an element of mass is accelerated only prior to its interaction with the tube walls. Considerable secondary experimental evidence, including streamline patterns, suggested that this model is valid. However, at the other extreme lies a model in which each mass element transfers momentum and energy to the walls as it is accelerated. The performance figures corresponding to this latter model are considerably inferior to those given in the text.

Interpretation of Results

One of the most significant results shown by Fig. 8 is the efficiency with which energy is transferred from the magnetic field to the plasma. Since 200 joules (corresponding to 160 kw) are transferred to the plasma, and 100 joules of these appear as useful axially directed kinetic energy, the transfer efficiency is 50%. As shown in the Appendix, this value is the usual theoretical limit for a constant phase velocity accelerator. One of the primary objectives of the program was to demonstrate a strong and efficient energy transfer with a magnetic induction engine.

A likewise significant feature is the energy lost to the walls. Half of the original 200 joules is eventually transferred to the walls. This undesirable result apparently stems, to an appreciable extent, from the action of the relatively weak transverse force components, which give the plasma a small radial velocity component. Once the plasma intercepts the wall as a result of this radial motion, there is a large amplification of the loss, because axially directed kinetic energy is transferred along with the radially directed energy. By the same reasoning, a modification that reduces the radial plasma motion even slightly may significantly improve the useful output of the engine.

The calorimetric efficiency of this engine, as shown in Fig. 8, is 50%; i.e., half of the total input energy to the plasma appears in the exhaust in one form or another. Even though a calorimetric efficiency of 50% is a respectable number for a plasma propulsion device at this time, one should be aware that all the energy caught is not useful directed energy and that the energy not caught is, in this engine at least, lost to the walls.

Finally, it is of interest to examine the performance figures that would exist for this engine *if* there were no interactions between the plasma and the walls; i.e., if the wall losses could be eliminated. These results are easily obtained, because the appropriate impulse is precisely what is measured by the drive-coil pendulum. The results for this hypothetical engine are roughly as follows: diameter, 5 cm; thrust, 2 newtons ($\frac{1}{2}$ lb); specific impulse, 5000 sec; plasma directed power, 80 kw; plasma total power, 160 kw; and plasma efficiency, 50%. The numbers really represent the engine's potential performance, which can be realized if the wall loss problem is overcome.

Future of the Transverse Induction Engine

The transverse-traveling-wave plasma engine has demonstrated a strong and efficient coupling between the magnetic field and the plasma, but at present the energy loss to the walls is prohibitive. The wall losses are believed to occur as a result of the relatively small transverse forces that inherently exist in the engine. Therefore, amelioration of these losses will probably require rather sophisticated techniques. However, one simple modification that may increase the engine's useful output appreciably is the elimination of the top and bottom of the propulsion tube. This modification would be expected to be fruitful if the wall loss amplification process mentioned earlier is correct. This unconfined geometry has not been tried because, in the present apparatus, the propulsion tube is part of the vacuum system.

Since the transverse force is alternating in nature, strong focusing methods familiar in particle accelerators may embody a solution. However, the perfection of techniques for focusing a continuous plasma will likely require a considerable developmental effort. Another approach is to change the mode of operation from that of an engine, with considerable slip between the plasma and the field, to a "hard-piston" engine with no slip. In an earlier pulsed version of the transverse induction engine with 3000 gauss, a no-slip operation existed with a spectroscopically pure exhaust plasma, indicating no wall interactions. The difficulty with the no-slip engine is its multimegawatt power level, which discouraged even laboratory testing on a continuous basis.

It has been noted that the present accelerator has essentially attained the theoretical limit of 50% efficiency for transferring energy from a constant-phase velocity magnetic field to an armature. However, it is demonstrated in the Appendix that greater theoretical efficiencies are available with a variable-phase velocity device. For example, it is shown that, assuming constant slip, 70% transfer efficiency appears to be attainable. Therefore, if a satisfactory solution to the wall loss problem is achieved, it would be worthwhile to construct a variable-phase velocity engine with the expectation of very efficient operation.

Appendix

A theoretical bound for the efficiency of a traveling-wave induction engine of constant-phase velocity is easily obtained as follows. One may visualize the traveling wave as being produced by a set of permanent magnets translating with the phase velocity V_f. This traveling field induces currents in the plasma which lead to forces accelerating the plasma in the direction of the traveling field. In a steady-state device, the accelerating force will be periodic (possibly constant).

Let V_0 be the velocity of the injected mass as it first enters the accelerating region and V_1 be the average velocity of the mass when its acceleration is completed. Let M be the mass injected in the time of one period T. Then the total momentum change in the plasma in one period is $M(V_1 - V_0)$. This is equal to the impulse delivered in one period by the drive assembly; namely,

$$\int_0^T F(t)\,dt$$

The energy delivered by the drive coil in one period E_{in} is

$$E_{\text{in}} = \int_0^T F(t)V_f dt = V_f \int_0^T F(t)dt$$

since V_f, the phase velocity, is constant; hence,

$$E_{\text{in}} = V_f M(V_1 - V_0)$$

To compute an efficiency for this engine, we compare this input energy to the minimum energy possible which will produce the same thrust. It is easily shown that the minimum energy possible arises when all the mass M is accelerated exactly to the average velocity V_1. Thus the minimum possible energy producing the same thrust is

$$E = \tfrac{1}{2}MV_1^2 - \tfrac{1}{2}MV_0^2$$

This gives the efficiency as

$$\eta = (\tfrac{1}{2}MV_1^2 - \tfrac{1}{2}MV_0^2)/[MV_f(V_1 - V_0)] = (V_1 + V_0)/2V_f$$

As an example, one observes that, if the injected mass is essentially at rest and is accelerated to the phase velocity, one has 50% efficiency as an upper limit.

The preceding bound depends only on rather general conditions, the essential one being that of constant-phase velocity. We shall now give a bound applicable to a nonconstant-phase velocity condition. In contrast to the preceding bound, that to be given depends on the details of the plasma motion during the acceleration process. Consequently, it is easier to phrase the bound in terms of the efficiency in accelerating discrete mass units, assuming no interaction with adjacent mass units, rather than in terms of the continuous flow used in the preceding case.

The case to be considered assumes that there is a constant-slip velocity S; that is, the difference between the field velocity V_f and the plasma velocity V_p is assumed to be constant: $V_f - V_p = S$. In the absence of wall interactions, the

accelerating force $F(t)$ on the plasma mass M is equal to the force on the traveling field. The plasma, assumed initially at rest, has velocity V_p given by

$$V_p(t) = \frac{1}{M}\int_0^t F(\tau)d\tau$$

The energy supplied by the traveling field is

$$\begin{aligned} E_{\text{in}} &= \int_0^t F(\tau)V_f(\tau)d\tau \\ &= \int_0^t F(\tau)[S + V_p(\tau)]d\tau \\ &= S\int_0^t F(\tau)d(\tau) + \frac{1}{M}\left[\int_0^t F(\tau)\int_0^\tau F(\mu)d\mu\right]d\tau \end{aligned}$$

Integration by parts yields

$$\begin{aligned} E_{\text{in}} &= S\int_0^t F(\tau)d(\tau) + \frac{1}{2M}\left[\int_0^t F(\tau)d\tau\right]^2 \\ &= MSV_p(t) + \tfrac{1}{2}M[V_p(t)]^2 \end{aligned}$$

Consequently, the efficiency η is

$$\eta = \frac{\frac{1}{2}MV_p^2}{MSV_p + \frac{1}{2}MV_p^2} = \frac{1}{1 + 2\,(S/V_p)}$$

As an example, if the slip velocity is one-fifth of the final plasma velocity, the efficiency is $\frac{5}{7} \cong 70\%$.

References

[1] Jones, R. E. and Palmer, R. W., "Traveling wave plasma engine program at NASA Lewis Research Center," *3rd Symposium on the Engineering Aspects of Magnetohydrodynamics* (Gordon and Breach Science Publishers, New York, 1964).

[2] Covert, E. E. and Haldeman, C. W., "The traveling wave pump," ARS J. **31**, 1252–1260 (1961); also Covert, E. E., Boedeker, L. R., and Haldeman, C. W., "Recent results of studies of the traveling wave pump," AIAA J. **2**, 1040 (1964).

[3] Janes, G. S., Dotson, I., and Wilson, T., "Momentum transfer through magnetic fields," *Proceedings of Third Symposium on Advanced Propulsion Concepts* (Gordon and Breach Science Publishers, New York, 1963), Vol. 1.

[4] Penfold, A. S., "Experimental results concerning the electromagnetic acceleration of plasma toroids," 4th Annual Air Force Office of Scientific Research Contractors Meeting on Ion and Plasma Acceleration (April 1961).

[5] Marshall, J., "Hydromagnetic plasma gun," *Plasma Acceleration*, edited by S. W. Kash (Stanford University Press, Stanford, Calif., 1960), p. 60.